Available online at www.sciencedirect.com

ScienceDirect

Procedia Engineering 120 (2015) 406 – 409

Procedia Engineering

www.elsevier.com/locate/procedia

EUROSENSORS 2015

Capacitive vs piezoresistive MEMS gyroscopes: a theoretical and experimental noise comparison

F. Giacci*, S. Dellea, G. Langfelder

Politecnico di Milano, Dipartimento di Elettronica, Informazione e Bioigegneria, via Ponzio 34/4, I-20133, Milano, Italy

Abstract

This work aims both at theoretically formalizing a comparison between piezoresistive (PZR) and capacitive (CAP) gyroscopes in terms of resolution limits, and at validating the predictions through experimental measurements on MEMS devices of both types. As predicted by the developed theory, PZR gyroscopes, well immune to parasitic capacitances and void of feedback resistance noise, show 10-fold better angle random walk (ARW) than CAP gyroscopes for the same nominal mode-split value, the same drive-motion amplitude and the same electronic noise density.

Peer-review under responsibility of the organizing committee of EUROSENSORS 2015

Keywords: MEMS gyroscopes, angle random walk, gyroscope noise, inertial sensors

1. Introduction

Micromachined (MEMS) gyroscopes based on piezoresistive nano-gauge sensing have potentialities of compactness, given the absence of large nested parallel-plate sensing cells. Capacitive sensing, the most widely adopted technique in consumer-grade MEMS gyroscopes [1, 2], suffers from few inherent issues: electronic noise is amplified by parasitic capacitances at the sense nodes; parallel plates used for Coriolis motion sensing determine a squeeze-film damping, with associated thermomechanical noise, that represents an unavoidable resolution limit; finally, a sensitivity-area trade off exists as the output signal is proportional to the parallel plates area. Recent works demonstrated rate gyroscopes based on Si nano-gauge resistive sensing [3, 4] with ARW in the order of few mdps/√Hz within an area of 0.42 mm^2. The use of these few-µm-long sensing beams, with sub-micrometric cross-section,

* Corresponding author: Federico Giacci, *Tel.:* +39-02-2399-3744. *E-mail address:* federico.giacci@polimi.it

Peer-review under responsibility of the organizing committee of EUROSENSORS 2015
doi:10.1016/j.proeng.2015.08.652

minimizes the area occupation. Besides, electronic noise is independent on the capacitive parasitics. Further, the absence of parallel plates results in a lower thermomechanical noise. Finally, their sensitivity is dependent only on alignment tolerance rather than on area occupation.

This work formalizes and validates these considerations with a theoretical prediction on noise contributions and an experimental comparison, with board-level electronics, between the two mentioned sensing principles. For the same drive motion amplitude, the measured ARW for the CAP device is 152 mdps/√Hz at 2.5 V biasing voltage of the sense capacitors; the PZR device shows a 4.2 mdps/√Hz ARW for a bridge biasing voltage of 0.3 V.

2. Processes and devices

Two gyroscopes are considered, both built in surface micromachining processes. Fig 1a shows the 22-µm-thick capacitive device, fabricated in the ThELMA process from ST Microelectronics [5]. Fig. 1b shows the 15-µm-thick piezoresistive device based on nano gauge readout, fabricated using the so-called M&NEMS process [6]. Nano gauges (see the detail in Fig. 1c) are obtained starting from a Silicon-on-Insulator wafer and using only common micromachining steps (reactive ion etching, ultraviolet lithography, dry hydrofluoric acid attacks…).

Both the devices rely on a decoupled topology [2-4], with anti-phase, comb-driven, external frames, connected through a tuning-fork. Drive-mode resonance frequencies are nominally set at about 20 kHz, with the sense-mode intentionally designed 1 kHz above, for mode-split operation.

The gyroscopes are operated through identical drive loops, controlling the drive motion amplitude to 4 µm. In the CAP device, the Coriolis force is transferred to differential sense frames, capacitively coupled to fixed electrodes. For the PZR device, the Coriolis force is transferred to a lever system that differentially stresses a pair of nano gauges. In both the devices, quadrature compensation electrodes can be used to null the quadrature error [7].

Fig. 1: SEM picture of (a) the capacitive and (b) the piezoresistive doubly-decoupled Z-axis gyroscopes used in this work, to scale. SEM details of a 5-µm-long nano-gauge with (250 nm)^2 cross-section are shown in (c).

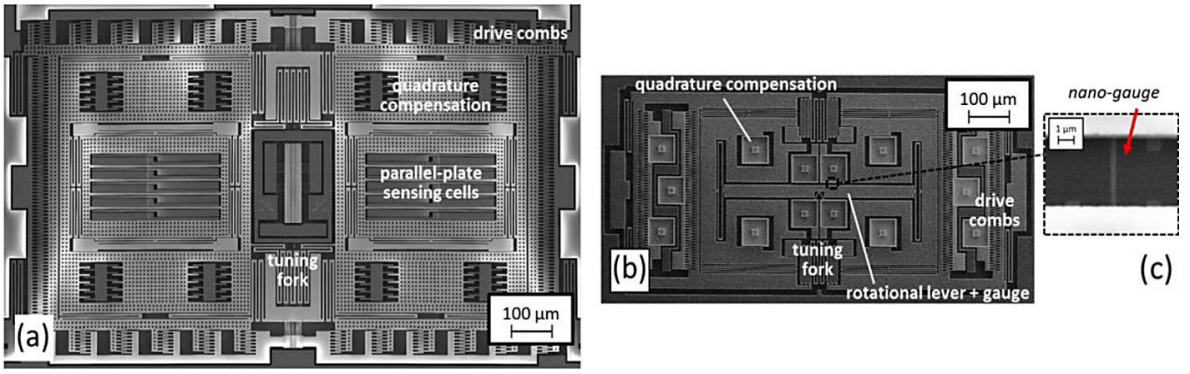

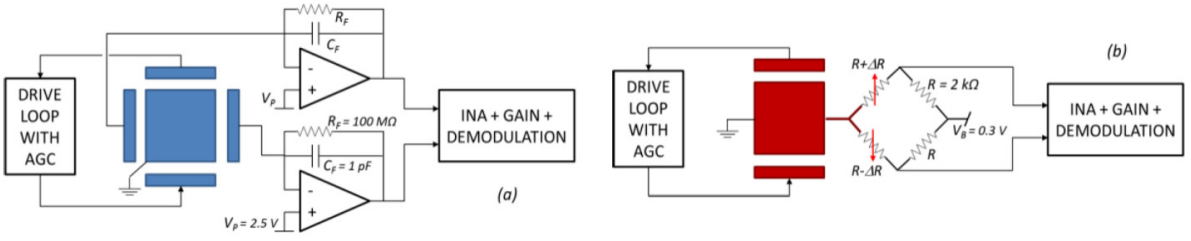

Fig. 2: block scheme of the board-level electronics used for the CAP (a) and PZR (b) gyroscope topologies. As highlighted, the sole difference is in the readout front-end interface, while both the AGC-controlled drive loop and the demodulation stages are identical.

3. Electronics

The devices are tested with board-level electronics (Fig. 2). The implemented drive circuit consists in a transimpedance-based oscillator, with feedthrough compensation, to excite the drive mode into resonant oscillation. In addition to this, a control electronics continuously monitors the drive displacement and adjusts the drive force to obtain the desired motion amplitude [4].

The block scheme of Fig. 2a also includes the board-level front-end of the CAP gyroscope, based on differential charge amplifiers. Similarly Fig. 2b shows the Wheatstone bridge used for the resistive sensing. The subsequent amplifying and demodulating stages are again identical.

4. Noise analysis and experimental results

In this section, the noise contributions for the systems shown in Fig. 2 are described. The PZR gyroscope is first affected by the thermomechanical noise of the Coriolis and sense frames, whose input-referred expression is:

$$S_{n.th} = \sqrt{\frac{k_b T b_s}{m_s^2 \omega_s^2 x_d^2}} \qquad (1)$$

where b_s is the sense damping coefficient; m_s the sense mass; ω_s the sense mode frequency in rad/s; x_d the drive displacement. k_b and T are the Boltzmann constant and absolute temperature. The resulting value, for a nominal package pressure of 1 mbar, is 1.3 mdps/√Hz. The Wheatstone bridge resistances *R* bring an overall Johnson noise:

$$S_{n,R,PZR} = \frac{2R}{V_b}\sqrt{4k_b TR}\,\frac{1}{\Delta R/\Delta\Omega} \qquad (2)$$

$\Delta R/\Delta\Omega$ is the sensitivity between rate and resistance variation [4]; the obtained value is 4.9 mdps/√Hz for a bridge biasing voltage V_b = 0.3 V. Due to their small cross section, the nano gauges also bring a 1/f noise contribution [8], which evaluated at the drive frequency, f_d turns out to be:

$$S_{n.1/f} = 2R\sqrt{\frac{\alpha}{4NL_g S_g f_d}}\,\frac{1}{\Delta R/\Delta\Omega} \qquad (3)$$

α is the Hooge coefficient, *N* the number of carriers in the resistor, S_g and L_g the section and length of the nano gauge, respectively. The resulting value is 0.8 mdps/√Hz. The electronic front-end contribution, represented by the instrumentation amplifier (INA) voltage noise density $S_{n,v,INA}$, contributes to the noise like the bridge resistances:

$$S_{n.,INA,PZR} = \frac{2R}{V_b}\sqrt{S_{n,v,INA}^2}\,\frac{1}{\Delta R/\Delta\Omega} \qquad (4)$$

This latter contribution is the dominant noise source, with a nominal value of 8.3mdps/√Hz. The overall noise, given by the quadratic sum of (1) to (4), turns out to be **9.7 mdps/√Hz** for the considered bridge biasing voltage.
Also the capacitive gyroscope is affected by a thermo-mechanical noise, with the same expression as (1). Though the much larger mass than for the PZR device and though the low nominal pressure of about 0.35 mbar, the larger damping coefficient determines a value (1 mdps/√Hz) similar to the PZR situation. The readout electronics relies on two charge amplifier stages, whose feedback resistances R_f give an overall input referred noise:

$$S_{n.,R,CAP} = \sqrt{\frac{8k_b T}{R_f}}\,\frac{1}{C_0}\,\frac{g_0}{V_p \omega_s}\,\frac{1}{x_d/\Delta\Omega} \qquad (5)$$

In the formula above g_0 is the parallel-plate gap; C_0 the single-ended sense capacitance at rest; $x_d/\Delta\omega$ is the scale factor between sense motion and angular rate [4]. The voltage V_P is 2.5 V, as in the following experimental results. The resulting value is 72.8 mdps/√Hz. Such a large value is mostly due to the discrete nature of the used resistances, and can be lowered in integrated circuits. The noise of the used operational amplifiers $S_{n,v,CA}$ = (10 nV/Hz)^2 is worsened

by the parasitic capacitance C_p affecting the virtual ground node, according to the following equation:

$$S_{n,\varphi\ln} = \sqrt{2S_{n,v,CA}^{\ 2}(1+\frac{C_p}{C_F})^2}\,\frac{C_F}{C_0}\frac{g_0}{V_p}\frac{1}{x_d/\Delta\Omega} \tag{6}$$

For a reasonable parasitic value of 10 pF, one gets 51.4 mdps/√Hz**.** Finally, the INA brings a noise contribution:

$$S_{n,,INA,CAP} = \sqrt{S_{n,v,INA}^{\ 2}}\,\frac{C_F}{C_0}\frac{g_0}{V_p}\frac{1}{x_d/\Delta\Omega} \tag{7}$$

resulting in a noise of 4.6 mdps/√Hz. The overall nominal noise turns out to be **89.2 mdps/√Hz**. Consumer gyroscopes can reach about one tenth of this value, basically by increasing the value of the integrated resistance (so decreasing the contribution in Eq. 5), and by increasing the biasing voltage V_p to values typically larger than 10 V. This latter approach however implies the use of charge pumps that contribute significantly to power dissipation.

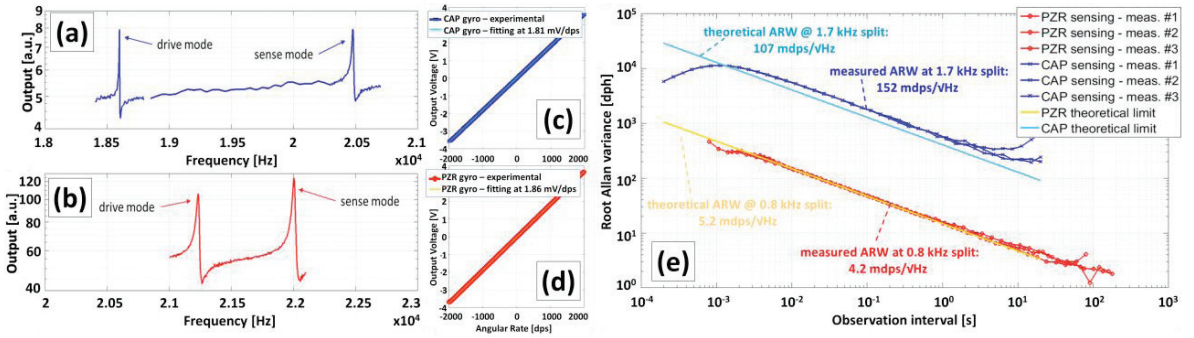

Fig. 3: summary of the obtained experimental results: characterization of the capacitive (a) and piezoresistive (b) gyroscopes drive and sense modes, showing a split of 1.7 kHz and 0.8 kHz respectively. Subfigures (c) and (d) reports the system output measurement: both the devices show 1.8 mV/dps on a ±2000 dps input, with linearity errors <5 ppm of the FSR. Finally, (e) reports the theoretical and experimental Allan variance, confirming the predictions (ARW derived from Allan graphs is by definition a factor √2 lower than corresponding white noise).

In operation, the devices show slightly different modes split (1700 Hz and 800 Hz for the CAP and PZR cases, see Fig. 3a-b). The sense chain gains are adjusted in order to achieve identical output sensitivity, as shown by Fig. 3c-d over a ±2000 dps rate. The measured ARW for the CAP device is 152 mdps/√Hz, 1.4-fold higher than the predictions corrected for the actual mismatch. This worsening is ascribed to parasitic capacitances larger than the 10-pF-value assumed Eq. (6). The PZR device shows a 4.2 mdps/√Hz ARW, matching the theoretical predictions for the true mismatch. These results, summarized by the Allan graph of Fig. 3e, confirm more than one order of magnitude better resolution for piezoresistive gyroscopes, though a 3-fold lower sense mass.

References

[1] L. Prandi et al., "A low-power 3-axis digital-output MEMS gyroscope with single drive and multiplexed angular rate readout," in Proc. IEEE Int. Solid-State Circuit Conf. (ISSCC), San Francisco, CA, USA, Feb. 2011, pp. 104–106.
[2] S. Lee et al., "Surface/bulk micromachined single-crystalline-silicon micro-gyroscope," J. Microelectromech. Syst., Vol. 9, n. 4, Dec 2000.
[3] S. Dellea, F. Giacci, A. Longoni, G. Langfelder, "In-Plane and Out-of-Plane MEMS Gyroscopes Based on Piezoresistive NEMS Detection," Journal of Microelectromechanical Systems, in press, DOI: 10.1109/JMEMS.2015.2441142.
[4] S. Dellea, F. Giacci, A. Longoni, P. Rey, A. Berthelot, and G. Langfelder, "Large full scale, linearity and cross-axis rejection in low-power 3-axis gyroscopes based on nanoscale piezoresistors," in Proc. IEEE 28th Int. Conf. MEMS, Estoril, Portugal, Jan. 2015, pp. 37–40.
[5] G. Langfelder, A. Longoni, A. Tocchio, E. Lasalandra, "MEMS motion sensors based on the variations of the fringe capacitances," IEEE Sensors Journal, Vol. 11, n. 4, 2011, pp. 1069-1077.
[6] Ph. Robert at al., "M&NEMS : A new approach for ultra-low cost 3D inertial sensor," in Proc. IEEE Sensors Conf., Christchurch, New Zealand, Oct. 2009, pp. 963–966.
[7] E. Tatar, S. E. Alper, and T. Akin, "Quadrature-error compensation and corresponding effects on the performance of fully decoupled MEMS gyroscopes," J. Microelectromech. Syst., vol. 21, no. 3, pp. 656–667, Jun. 2012.
[8] A.Walther et al., "3-axis gyroscope with Si nanogage piezo-resistive detection," proc. IEEE MEMS 2012 pp.480,483, Jan. 29-Feb. 2 2012.